PERGAMON

International Journal of Heat and Mass Transfer 45 (2002) 2673–2688

International Journal of HEAT and MASS TRANSFER

www.elsevier.com/locate/ijhmt

Simultaneous radiation and conduction heat transfer in a graded index semitransparent slab with gray boundaries

Xin-Lin Xia, Yong Huang *, He-Ping Tan, Xiao-Bin Zhang

School of Energy Science and Engineering, Harbin Institute of Technology, 92 West Dazhi Street, Harbin, Hei Longjiang 150001, People's Republic of China

Received 2 November 2001

Abstract

The simultaneous radiation and conduction heat transfer in a semitransparent slab of absorbing–emitting gray medium is solved in this paper. The refractive index of the medium spatially varies in a linear relationship, and the two boundary walls are diffuse and gray. A curved ray tracing technique in combination with a pseudo-source adding method is employed to deduce the radiative intensities on gray walls. Resorting to some of the results presented by Ben Abdallah and Le Dez, an exact expression of the radiative flux in medium is deduced. The influences on the temperature and radiative flux fields are examined, which are caused by the refractive index distribution, absorbing coefficient, thermal conductivity and the boundary wall emissivities. The results display the significant influences of the refractive index distribution and boundary wall emissivities on the radiative flux and temperature in medium. © 2002 Published by Elsevier Science Ltd.

Keywords: Simultaneous radiation and conduction heat transfer; Graded index; Semitransparent medium; Curved ray tracing method; Pseudo-source adding method

1. Introduction

The refractive index has significant influences on the raditive transfer in medium. Spuckler and Siegel [1–3] analyzed the refractive index effects on the radiative transfer in a single layer of semitransparent medium and in multilayered regions. Tan and Wang et al. [4] investigated the coupled radiation and conduction heat transfer in a composite of several semitransparent layers, each with respective constant refractive index. The material structure, the thermal effect and some others can result in inhomogeneous refractive index distribution in medium, which is usually called the graded index (GRIN), and often plays important part effect on the phenomena and physical process [5]. Recently, Ben Abdallah and Le Dez [6,7] investigated the radiative transfer and the combined radiative and conductive heat transfer in a GRIN semitransparent slab, they developed a curved ray tracing technique to analyze the radiative transfer inside the medium with two black walls. The temperature and heat flux distributions are reported to show that the GRIN in a semitransparent medium can greatly influence the inside temperature distribution and heat flux field, as well as the apparent emission emerging from its surface [8,9].

In this paper, the pseudo-source adding method [10] is employed in combination with the curved ray tracing technique to solve the radiative transfer in medium characterized by a linear refractive index distribution. Instead of black boundaries, two diffuse and gray walls are considered. And resorting to some investigation results reported by Ben Abdallah and Le Dez [8,9], the temperature and radiative flux distributions inside an absorbing–emitting slab of GRIN gray medium are solved for the simultaneous radiation and conduction heat transfer.

* Corresponding author. Tel.: +86-451-641-2148.
E-mail address: huangy_zl@263.net (Y. Huang).

0017-9310/02/$ - see front matter © 2002 Published by Elsevier Science Ltd.
PII: S0017-9310(01)00367-2

Nomenclature

a_k	reduced refractive index at upside of mesh k, $a_k = \frac{1}{2}(\bar{n}_k + \bar{n}_{k+1})$
A_k	coefficients for discretization
b_k	reduced refractive index at downside of mesh k, $b_k = \frac{1}{2}(\bar{n}_k + \bar{n}_{k-1})$
B_{kj}, B'_{kj}	coefficients for discretization
C_k	coefficients for discretization
d	slab thickness, m
$E_n(x)$	nth-order exponential integral function
I	radiative intensity, W/m^2 sr
I_m	radiative intensity of medium, W/m^2 sr
k	influence factor
K	process extinction coefficient
n	refractive index
$\bar{n}$	reduced refractive index, $\bar{n}(z) = n(z)/n_2$
N	number of meshes
q	heat flux density, W/m^2
s	spatial position
T	temperature, K
z	space coordinate, m

Greek symbols

ε	emissivity of boundary wall
ζ	polar angle
κ	absorption coefficient, m^{-1}
λ	conductivity, W/m K
μ	directional cosine
ξ	incident angle on boundary 2
ξ'	incident angle on boundary 1
σ	Stefan–Boltzmann constant, W/m^2 K^4
$\bar{\tau}$	generalized optical thickness, $\bar{\tau} = (\kappa d n_2)/(n_1 - n_2)$
Ω	spatial direction

Superscripts and subscripts

+, −	direction from boundary 1 to boundary 2 (+) or from boundary 2 to boundary 1 (−)
1, 2	boundary 1, boundary 2
b	boundary wall, or black body
c	conduction
j, k	mesh order
p	pseudo-source
r	radiation

2. Geometrical and physical model

Consider an infinite parallel plane slab of absorbing–emitting but nonscattering gray medium of thickness d, as illustrated in Fig. 1. The emissivities of the two diffuse gray boundary walls are ε_1 and ε_2, and the temperatures are T_{b1} and T_{b2}, respectively. The medium is characterized by a constant absorption coefficient κ and a refractive index $n(z)$ spatially varying in a linear relationship below.

$$n(z) = n_2 + (n_1 - n_2)z/d, \tag{1}$$

where n_1 and n_2 are refractive index values of the medium adjacent to the two boundary walls, respectively.

A steady-state temperature field $T(x)$ in medium, caused by the simultaneous radiation and conduction heat transfer, is considered only for the case of $n_1 > n_2$ below, but the results will be also valid for the case of $n_1 < n_2$.

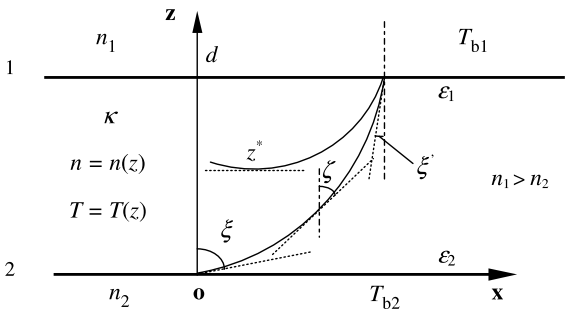

Fig. 1. Schematic diagram of geometrical and physical model.

3. Radiative flux in medium

3.1. Radiative flux in medium with black boundaries

The radiative flux inside the medium can be expressed as

$$q_r(s) = \int_{\Omega=4\pi} I_{\mathrm{m}}(s,\Omega)\Omega\,\mathrm{d}\Omega, \tag{2}$$

where $I_{\mathrm{m}}(s,\Omega)$ is the radiative intensity of medium at position s and in direction Ω. For a one-dimensional infinite slab, the azimuthal symmetry leads to

$$\int_{\Omega=2\pi} I_{\mathrm{m}}(s,\Omega)\Omega\,\mathrm{d}\Omega = 2\pi\int_{\mu=0}^{1}[I_{\mathrm{m}}(z,\mu)-I_{\mathrm{m}}(z,-\mu)]\mu\,\mathrm{d}\mu, \tag{3}$$

where $\mu=\cos\zeta$ is the cosine of the angle between the z-axis and the propagating direction of the radiation intensity.

For a slab of medium with black boundaries and a linear refractive index distribution, the incoming intensities at a point z inside the medium have been derived by Ben Abdallah and Le Dez [7]. And an exact expression for the radiative flux inside the medium was obtained [9] as

$$\begin{aligned}
\frac{q_{rz}(z)}{2\sigma n^2(z)} = {} & T_{\mathrm{b2}}^4\int_{\mu=\frac{\sqrt{\bar n^2(z)-1}}{\bar n(z)}}^{1}\exp\left(-\bar\tau\bar n(z)\left[\mu-\sqrt{\mu^2+\frac{1-\bar n^2(z)}{\bar n^2(z)}}\right]\right)\mu\,\mathrm{d}\mu \\
& + T_{\mathrm{b1}}^4\left\{\int_{\mu=0}^{\frac{\sqrt{\bar n^2(z)-1}}{\bar n(z)}}\exp\left(-\bar\tau\bar n(z)\left[\mu+\sqrt{\mu^2+\frac{\bar n^2(d)-\bar n^2(z)}{\bar n^2(z)}}\right]\right)\mu\,\mathrm{d}\mu\right. \\
& \left. -\int_{\mu=0}^{1}\exp\left(-\bar\tau\bar n(z)\left[\sqrt{\mu^2+\frac{\bar n^2(d)-\bar n^2(z)}{\bar n^2(z)}}-\mu\right]\right)\mu\,\mathrm{d}\mu\right\} \\
& + \kappa\int_{\mu=\frac{\sqrt{\bar n^2(z)-1}}{\bar n(z)}}^{1}\int_{z'=0}^{z}\frac{\bar n(z')T^4(z')\exp\left(-\bar\tau\bar n(z)\left[\mu-\sqrt{\mu^2+\frac{\bar n^2(z')-\bar n^2(z)}{\bar n^2(z)}}\right]\right)}{\bar n(z)\sqrt{\mu^2+\frac{\bar n^2(z')-\bar n^2(z)}{\bar n^2(z)}}}\,\mathrm{d}z'\,\mu\,\mathrm{d}\mu \\
& - \kappa\int_{\mu=0}^{1}\int_{z'=z}^{d}\frac{\bar n(z')T^4(z')\exp\left(-\bar\tau\bar n(z)\left[\sqrt{\mu^2+\frac{\bar n^2(z')-\bar n^2(z)}{\bar n^2(z)}}-\mu\right]\right)}{\bar n(z)\sqrt{\mu^2+\frac{\bar n^2(z')-\bar n^2(z)}{\bar n^2(z)}}}\,\mathrm{d}z'\,\mu\,\mathrm{d}\mu \\
& + \kappa\int_{\mu=0}^{\frac{\sqrt{\bar n^2(z)-1}}{\bar n(z)}}\left\{\int_{z'=z^*(\mu)}^{z}\frac{\bar n(z')T^4(z')\exp\left(-\bar\tau\bar n(z)\left[\mu-\sqrt{\mu^2+\frac{\bar n^2(z')-\bar n^2(z)}{\bar n^2(z)}}\right]\right)}{\bar n(z)\sqrt{\mu^2+\frac{\bar n^2(z')-\bar n^2(z)}{\bar n^2(z)}}}\,\mathrm{d}z'\right. \\
& \left. + \int_{z'=z^*(\mu)}^{d}\frac{\bar n(z')T^4(z')\exp\left(-\bar\tau\bar n(z)\left[\mu+\sqrt{\mu^2+\frac{\bar n^2(z')-\bar n^2(z)}{\bar n^2(z)}}\right]\right)}{\bar n(z)\sqrt{\mu^2+\frac{\bar n^2(z')-\bar n^2(z)}{\bar n^2(z)}}}\,\mathrm{d}z'\right\}\mu\,\mathrm{d}\mu,
\end{aligned} \tag{4}$$

where T is the absolute temperature, $\bar n(z)=n(z)/n_2$ is the reduced refractive index and $\bar\tau=(\kappa d n_2)/(n_1-n_2)$ is the generalized optical thickness.

If two temperatures T_{p1} and T_{p2}, determined by considering the gray boundary effect, are employed to replace the boundary temperatures T_{b1} and T_{b2} in Eq. (4), then the expression will be valid for a slab of medium with a linear refractive index distribution and gray boundaries.

3.2. Radiative intensities leaving gray boundary walls

The radiative intensity leaving a gray boundary is the combination of the wall emission and reflection. The pseudo-source adding method can be employed to solve the radiative intensity leaving a gray boundary.

3.2.1. Radiative intensities $I^+(d,\xi')$ and $I^-(0,\xi)$

We introduce $I^+(d,\xi')$ and $I^-(0,\xi)$ to represent the respective radiative intensities incoming on boundary 1 and boundary 2, without considering the emission or reflection of the boundary walls are included. The symbols ξ' and ξ denote the incident angles on boundary 1 and boundary 2, respectively.

The radiative transfer equation in a GRIN medium is

$$\frac{\mathrm{d}}{\mathrm{d}s}\left[\frac{I(s,\Omega)}{n^2(s)}\right]+\kappa(s)\frac{I(s,\Omega)}{n^2(s)}=\kappa(s)I_{\mathrm{b}}(s). \tag{5}$$

For a ray originating from a point of $z=0$, the curvilinear abscissa on its trajectory is [8]

$$s(z)=\frac{d}{n_1-n_2}\left[\sqrt{n^2(z)-n_2\sin^2\xi}-n_2\cos\xi\right]=\frac{\bar{\tau}}{\kappa}\left[\sqrt{\bar{n}^2(z)-\sin^2\xi}-\cos\xi\right], \tag{6}$$

where $\bar{\tau}=\tau n_2/(n_1-n_2)=\kappa d n_2/(n_1-n_2)$ and $\bar{n}(z)=n(z)/n_2$. Hence,

$$\mathrm{d}s=\frac{\bar{n}(z)}{\sqrt{\bar{n}^2(z)-\sin^2\xi}}\,\mathrm{d}z. \tag{7}$$

While for that originating from a point of $z=d$, the curvilinear abscissa on the trajectory is

$$s(z)=\frac{d}{n_1-n_2}\left[\sqrt{n^2(z)-n_1\sin^2\xi'}-n_1\cos\xi'\right]=\frac{\bar{\tau}}{\kappa}\left[\sqrt{\bar{n}^2(z)-\bar{n}^2(d)\sin^2\xi'}-\bar{n}(d)\cos\xi'\right]. \tag{8}$$

So,

$$\mathrm{d}s=\frac{\bar{n}(z)}{\sqrt{\bar{n}^2(z)-\bar{n}(d)\sin^2\xi'}}\,\mathrm{d}z. \tag{9}$$

Integrating Eq. (5) and considering Eqs. (6) and (7), we have

$$I^-(0,\xi)=n_2^2\int_0^{s(d)}\kappa(s)I_{\mathrm{b}}(s)\exp\left[-\int_0^s\kappa(s')\,\mathrm{d}s'\right]\mathrm{d}s=\kappa n_2^2\int_0^d\bar{n}(z)I_{\mathrm{b}}(z)\frac{\exp\left[\bar{\tau}\cos\xi-\bar{\tau}\sqrt{\bar{n}^2(z)-\sin^2\xi}\right]}{\sqrt{\bar{n}^2(z)-\sin^2\xi}}\,\mathrm{d}z. \tag{10}$$

For a ray incidence on boundary 1, if $\xi'\leqslant\arcsin(n_2/n_1)$, boundary 2 can be reached by tracing its trajectory in the reverse direction. Integrating Eq. (5) and utilizing Eqs. (8) and (9), it can give

$$\begin{aligned}I^+(d,\xi')&=n_1^2\int_{s(0)}^{s(d)}\kappa(s)I_{\mathrm{b}}(s)\exp\left[-\int_s^{s(d)}\kappa(s')\,\mathrm{d}s'\right]\mathrm{d}s\\&=\kappa n_1^2\int_0^d\bar{n}(z)I_{\mathrm{b}}(z)\frac{\exp\left[-\bar{\tau}\bar{n}(d)\cos\xi'+\bar{\tau}\sqrt{\bar{n}^2(z)-\bar{n}^2(d)\sin^2\xi'}\right]}{\sqrt{\bar{n}^2(z)-\bar{n}^2(d)\sin^2\xi'}}\,\mathrm{d}z.\end{aligned} \tag{11}$$

However, when $\xi'>\arcsin(n_2/n_1)$, tracing its trajectory in the reverse direction can return back to boundary 1 instead of boundary 2, because of the total reflection at point $z^*=(\bar{\tau}/\kappa)[1-\bar{n}(d)\sin\xi']$. By integrating Eq. (5) with considering the integral limit change and utilizing Eqs. (8) and (9), it can be deduced as

$$
\begin{aligned}
I^+(d,\xi') = {} & n_1^2\int_{s(z^*)}^{s(d)}\kappa(s)I_b(s)\exp\left[-\int_s^{s(d)}\kappa(s')\,ds'\right]ds + n_1^2\int_{s(z^*)}^{s(d)}\kappa(s)I_b(s)\\
& \times\exp\left[-\int_{s(z^*)}^{s(d)}\kappa(s')\,ds' - \int_{s(z^*)}^{s}\kappa(s')\,ds'\right]ds\\
= {} & \kappa n_1^2\int_{z^*}^{d}\bar{n}(z)I_b(z)\frac{\exp\left[-\bar{\tau}\bar{n}(d)\cos\xi' + \bar{\tau}\sqrt{\bar{n}^2(z)-\bar{n}^2(d)\sin^2\xi'}\right]}{\sqrt{\bar{n}^2(z)-\bar{n}^2(d)\sin^2\xi'}}\,dz\\
& + \kappa n_1^2\int_{z^*}^{d}\bar{n}(z)I_b(z)\frac{\exp\left[-\bar{\tau}\bar{n}(d)\cos\xi' - \bar{\tau}\sqrt{\bar{n}^2(z)-\bar{n}^2(d)\sin^2\xi'}\right]}{\sqrt{\bar{n}^2(z)-\bar{n}^2(d)\sin^2\xi'}}\,dz. \qquad (12)
\end{aligned}
$$

3.2.2. Combined radiative intensity

The reflected radiation energy on a diffuse gray boundary wall, will act in combination with the emitted energy from it. The combined radiative intensities I_{0p1} and I_{0p2} are introduced for two boundaries 1 and 2, respectively.

Integrating $I^+(d,\xi')$ over the hemispherical space to get the total incident energy on boundary 1, and the combined radiative intensity I_{0p1} can be expressed as

$$
\begin{aligned}
I_{0p1} = {} & 2(1-\varepsilon_1)\int_0^{\pi/2} I^+(d,\xi')\sin\xi'\cos\xi'\,d\xi' + n_1^2\varepsilon_1\sigma T_{t1}^4\\
= {} & 2(1-\varepsilon_1)n_1^2\int_{\sqrt{\frac{\bar{n}^2(d)-1}{\bar{n}(d)}}}^{1}\int_0^{d}\kappa\bar{n}(z)I_b(z)\mu\frac{\exp\left[-\bar{\tau}\bar{n}(d)\mu + \bar{\tau}\sqrt{\bar{n}^2(z)-\bar{n}^2(d)(1-\mu^2)}\right]}{\sqrt{\bar{n}^2(z)-\bar{n}^2(d)(1-\mu^2)}}\,dz\,d\mu\\
& + 4(1-\varepsilon_1)n_1^2\int_0^{\sqrt{\frac{\bar{n}^2(d)-1}{\bar{n}(d)}}}\int_{z^*}^{d}\kappa\bar{n}(z)I_b(z)\mu\frac{\exp\left[-\bar{\tau}\bar{n}(d)\mu\right]\mathrm{ch}\left[\bar{\tau}\sqrt{\bar{n}^2(z)-\bar{n}^2(d)(1-\mu^2)}\right]}{\sqrt{\bar{n}^2(z)-\bar{n}^2(d)(1-\mu^2)}}\,dz\,d\mu + n_1^2\varepsilon_1\sigma T_{t1}^4/\pi
\end{aligned} \qquad (13)
$$

and the relationship between z and μ can lead to a transformation, which is

$$
\begin{aligned}
& \int_{\mu=0}^{\sqrt{\frac{\bar{n}^2(d)-1}{\bar{n}(d)}}}\int_{z^*}^{d}\kappa\bar{n}(z)I_b(z)\mu\frac{\exp\left[-\bar{\tau}\bar{n}(d)\mu\right]\mathrm{ch}\left[\bar{\tau}\sqrt{\bar{n}^2(z)-\bar{n}^2(d)(1-\mu^2)}\right]}{\sqrt{\bar{n}^2(z)-\bar{n}^2(d)(1-\mu^2)}}\,dz\,d\mu\\
= {} & \int_{z=0}^{d}\int_{\sqrt{\frac{\bar{n}^2(d)-\bar{n}^2(z)}{\bar{n}(d)}}}^{\sqrt{\frac{\bar{n}^2(d)-1}{\bar{n}(d)}}}\kappa\bar{n}(z)I_b(z)\mu\frac{\exp\left[-\bar{\tau}\bar{n}(d)\mu\right]\mathrm{ch}\left[\bar{\tau}\sqrt{\bar{n}^2(z)-\bar{n}^2(d)(1-\mu^2)}\right]}{\sqrt{\bar{n}^2(z)-\bar{n}^2(d)(1-\mu^2)}}\,d\mu\,dz. \qquad (14)
\end{aligned}
$$

Hence, Eq. (13) can be rewritten as

$$
\begin{aligned}
I_{0p1} = {} & 2(1-\varepsilon_1)n_1^2\int_{z=0}^{d}\int_{\sqrt{\frac{\bar{n}^2(d)-\bar{n}^2(z)}{\bar{n}(d)}}}^{1}\kappa\bar{n}(z)I_b(z)\mu\frac{\exp\left[-\bar{\tau}\bar{n}(d)\mu + \bar{\tau}\sqrt{\bar{n}^2(z)-\bar{n}^2(d)(1-\mu^2)}\right]}{\sqrt{\bar{n}^2(z)-\bar{n}^2(d)(1-\mu^2)}}\,d\mu\,dz\\
& + 2(1-\varepsilon_1)n_1^2\int_{z=0}^{d}\int_{\sqrt{\frac{\bar{n}^2(d)-\bar{n}^2(z)}{\bar{n}(d)}}}^{\sqrt{\frac{\bar{n}^2(d)-1}{\bar{n}(d)}}}\kappa\bar{n}(z)I_b(z)\mu\frac{\exp\left[-\bar{\tau}\bar{n}(d)\mu - \bar{\tau}\sqrt{\bar{n}^2(z)-\bar{n}^2(d)(1-\mu^2)}\right]}{\sqrt{\bar{n}^2(z)-\bar{n}^2(d)(1-\mu^2)}}\,d\mu\,dz\\
& + n_1^2\varepsilon_1\sigma T_{t1}^4/\pi. \qquad (15)
\end{aligned}
$$

Similarly, integrating $I^-(0,\xi)$ over the hemispherical space, the total incidence energy on boundary 2 can be obtained and the combined radiative intensity will be

$$I_{0p2} = 2(1-\varepsilon_2)\int_0^{\pi/2} I^-(0,\xi)\sin\xi\cos\xi\,\mathrm{d}\xi + n_2^2\varepsilon_2\sigma T_{t2}^4$$
$$= 2(1-\varepsilon_2)n_2^2\int_0^1\int_0^d \kappa\bar{n}(z)I_b(z)\mu\frac{\exp\left[\bar{\tau}\mu-\bar{\tau}\sqrt{\bar{n}^2(z)-1+\mu^2}\right]}{\sqrt{\bar{n}^2(z)-1+\mu^2}}\,\mathrm{d}z\,\mathrm{d}\mu + n_2^2\varepsilon_2\sigma T_{t2}^4/\pi. \tag{16}$$

By the above deductions, the medium emission has been transformed to be included in the combined radiation from the two boundaries. Thus, the absorbing–emitting medium can be dealt with as an absorbing one in the following way.

3.2.3. The first pseudo-source intensity

The combined radiative intensity I_{0p2} from boundary 2 propagates through the medium to reach boundary 1, and then is reflected there. On boundary 1, the reflected intensity will act together with the combined radiative intensity I_{0p1}, their sum is denoted by I_{1p1} and named as the first pseudo-source intensity from boundary 1. Similarly, the combined radiative intensity I_{0p1} from boundary 1 propagates through the medium to reach boundary 2 and then is reflected. The sum of the reflected intensity and the combined radiative intensity I_{0p2} on boundary 2 is denoted by I_{1p2} and named as the first pseudo-source intensity from boundary 2. Then, the following expressions can be found:

$$I_{1p1} = I_{0p1} + I_{0p2}k_2(1-\varepsilon_1), \tag{17}$$

$$I_{1p2} = I_{0p2} + I_{0p1}k_1(1-\varepsilon_2), \tag{18}$$

where k_1 and k_2 are the influencing factors of the two boundary walls, as

$$k_1 = \frac{\int_0^{\arcsin(n_2/n_1)} 2\exp\left[-\int_{s(0)}^{s(d)}\kappa(s)\,\mathrm{d}s\right]\sin\xi'\cos\xi'\,\mathrm{d}\xi'}{1-(1-\varepsilon_1)\int_{\arcsin(n_2/n_1)}^{\pi/2} 2\exp\left[-2\int_{s(z^*)}^{s(d)}\kappa(s)\,\mathrm{d}s\right]\sin\xi'\cos\xi'\,\mathrm{d}\xi'}$$
$$= \frac{(1/\bar{n}^2(d))\int_0^1 2\mu\exp\left[\bar{\tau}\mu-\bar{\tau}\sqrt{\mu^2+\bar{n}^2(d)-1}\right]\mathrm{d}\mu}{1-(1-\varepsilon_1)\int_0^{\frac{\sqrt{\bar{n}^2(d)-1}}{\bar{n}(d)}} 2\mu\exp\left[-2\bar{\tau}\bar{n}(d)\mu\right]\mathrm{d}\mu}, \tag{19}$$

$$k_2 = \int_0^{\pi/2} 2\exp\left[-\int_{s(0)}^{s(d)}\kappa(s)\,\mathrm{d}s\right]\sin\xi\cos\xi\,\mathrm{d}\xi = \int_0^1 2\mu\exp\left[\bar{\tau}\mu-\bar{\tau}\sqrt{\mu^2+\bar{n}^2(d)-1}\right]\mathrm{d}\mu. \tag{20}$$

The two formulae above can be finally reduced as

$$k_2 = \frac{\left[\bar{n}^2(d)+1\right]^2}{2}E_3\left[\bar{\tau}\bar{n}(d)-\bar{\tau}\right] - \frac{\bar{n}^2(d)-1}{2}E_3\left[\bar{\tau}\sqrt{\bar{n}^2(d)-1}\right] + \frac{\bar{\tau}\sqrt{\bar{n}^2(d)-1}+1}{2\bar{\tau}^2}\mathrm{e}^{-\bar{\tau}\sqrt{\bar{n}^2(d)-1}}$$
$$-\frac{\bar{\tau}\left[\bar{n}(d)-1\right]+1}{2\bar{\tau}^2}\mathrm{e}^{-\bar{\tau}\left[\bar{n}(d)-1\right]}, \tag{21}$$

$$k_1 = (k_2/\bar{n}^2(d))\Bigg/\left\{1-(1-\varepsilon_1)\frac{1-\left[1+2\bar{\tau}\sqrt{\bar{n}^2(d)-1}\right]\mathrm{e}^{-2\bar{\tau}\sqrt{\bar{n}^2(d)-1}}}{2\bar{\tau}^2\bar{n}^2(d)}\right\}, \tag{22}$$

where $E_n(x)$ is a nth-order exponential integral function.

3.2.4. Radiative intensities leaving gray boundary walls

The radiative energy leaving a boundary wall can partly return back to it after propagating through the medium and being reflected by the other boundary. A process extinction coefficient, k, is introduced here to represent the quotient of

the returning energy to that leaving a boundary, i.e., K_1 and K_2 for boundary 1 and boundary 2, respectively. The following expressions can be derive for them:

$$\begin{aligned} K_1 &= (1-\varepsilon_2)k_2^2/\bar{n}^2(d) + \int_{\arcsin(n_2/n_1)}^{\pi/2} 2\exp\left[-2\int_{s(z^*)}^{s(d)}\kappa(s)\,\mathrm{d}s\right]\sin\xi'\cos\xi'\,\mathrm{d}\xi' \\ &= (1-\varepsilon_2)k_2^2/\bar{n}^2(d) + \int_{\arcsin(n_2/n_1)}^{\pi/2} 2\exp\left[-2\bar{\tau}\bar{n}(d)\cos\xi'\right]\sin\xi'\cos\xi'\,\mathrm{d}\xi' \\ &= (1-\varepsilon_2)k_2^2/\bar{n}^2(d) + \int_0^{\frac{\sqrt{\bar{n}^2(d)-1}}{\bar{n}(d)}} 2\mu\exp\left[-2\bar{\tau}\bar{n}(d)\mu\right]\mathrm{d}\mu \\ &= (1-\varepsilon_2)k_2^2/\bar{n}^2(d) + \frac{1-\left[1+2\bar{\tau}\sqrt{\bar{n}^2(d)-1}\right]\mathrm{e}^{-2\bar{\tau}\sqrt{\bar{n}^2(d)-1}}}{2\bar{\tau}^2\bar{n}^2(d)}, \end{aligned} \tag{23}$$

$$\begin{aligned} K_2 &= \frac{(1-\varepsilon_1)k_2^2/\bar{n}^2(d)}{1-(1-\varepsilon_1)\int_{\arcsin(n_2/n_2)}^{\pi/2} 2\exp\left[-2\int_{s(z^*)}^{s(d)}\kappa(s)\,\mathrm{d}s\right]\sin\xi'\cos\xi'\,\mathrm{d}\xi'} \\ &= \frac{(1-\varepsilon_1)k_2^2/\bar{n}^2(d)}{1-(1-\varepsilon_1)\int_0^{\frac{\sqrt{\bar{n}^2(d)-1}}{\bar{n}(d)}} 2\mu\exp\left[-2\bar{\tau}\bar{n}(d)\mu\right]\mathrm{d}\mu} = \frac{(1-\varepsilon_1)k_2^2/\bar{n}^2(d)}{1-(1-\varepsilon_1)\frac{1-\left[1+2\bar{\tau}\sqrt{\bar{n}^2(d)-1}\right]\mathrm{e}^{-2\bar{\tau}\sqrt{\bar{n}^2(d)-1}}}{2\bar{\tau}^2\bar{n}^2(d)}}. \end{aligned} \tag{24}$$

The radiative intensity leaving a boundary wall is the comprehensive contributions of medium emission and absorption as well as the boundary wall emission and reflection. I_1 and I_2 are introduced to denote the radiative intensities leaving the two boundaries, respectively, and we have

$$I_1 = \frac{I_{1\mathrm{p}1}}{1-K_1(1-\varepsilon_1)}, \tag{25}$$

$$I_2 = \frac{I_{1\mathrm{p}2}}{1-K_2(1-\varepsilon_2)}. \tag{26}$$

The radiative intensities I_1 and I_2 can be regarded as that emitted from two pseudo-black walls with temperatures of $T_{\mathrm{p}1}$ and $T_{\mathrm{p}2}$, respectively, which are

$$T_{\mathrm{p}1} = \sqrt[4]{\frac{\pi I_1}{\sigma n_1^2}}, \tag{27}$$

$$T_{\mathrm{p}2} = \sqrt[4]{\frac{\pi I_2}{\sigma n_2^2}}. \tag{28}$$

3.3. Solution to radiative flux in medium

The medium is cut out into isothermal slices labeled k, of equal depth Δz and with center z_k, for $2 \leqslant k \leqslant N-1$, N being the total number of meshes (gray interfaces included), as illustrated in Fig. 2. Thus, $I_{0\mathrm{p}1}$ can be exactly calculated for a linear refractive index, leading to the formal expression

$$I_{0\mathrm{p}1} = \frac{n_1^2\sigma}{\pi}\sum_{k=1}^{N} A_k T_k^4, \tag{29}$$

where $T_1 = T_{\mathrm{b}2}$, $T_N = T_{\mathrm{b}1}$, $A_1 = 0$ and $A_N = \varepsilon_1$. For $2 \leqslant k \leqslant N-1$, A_k is

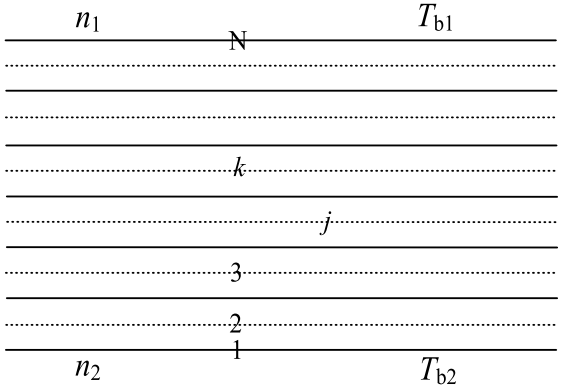

Fig. 2. Discretization of the slab.

$$
\begin{aligned}
A_k = 2(1-\varepsilon_1)\Bigg\{ & \bar{\tau}E_3\Big[\bar{\tau}(\bar{n}_d - a_k)\Big] - \bar{\tau}E_3\Big[\bar{\tau}(\bar{n}_d - b_k)\Big] - \frac{E_5\Big[\bar{\tau}(\bar{n}_d - a_k)\Big] - E_5\Big[\bar{\tau}(\bar{n}_d - b_k)\Big]}{\bar{\tau}^2\bar{n}_d^2} \\
& + \frac{(a_k - \bar{\tau}\bar{n}_d)E_4\Big[\bar{\tau}(\bar{n}_d - a_k)\Big] - (b_k - \bar{\tau}\bar{n}_d)E_4\Big[\bar{\tau}(\bar{n}_d - b_k)\Big]}{\bar{\tau}\bar{n}_d^2} \\
& + \frac{E_4\Big[\bar{\tau}(\sqrt{\bar{n}_d^2-1} + \sqrt{a_k^2-1})\Big] - E_4\Big[\bar{\tau}(\sqrt{\bar{n}_d^2-1} + \sqrt{b_k^2-1})\Big]}{\bar{\tau}^2\bar{n}_d^2/\sqrt{\bar{n}_d^2-1}} \\
& + \frac{E_5\Big[\bar{\tau}(\sqrt{\bar{n}_d^2-1} + \sqrt{a_k^2-1})\Big] - E_5\Big[\bar{\tau}(\sqrt{\bar{n}_d^2-1} + \sqrt{b_k^2-1})\Big]}{\bar{\tau}^2\bar{n}_d^2} \\
& + \frac{\sqrt{a_k^2-1}E_3\Big[\bar{\tau}(\sqrt{\bar{n}_d^2-1} + \sqrt{a_k^2-1})\Big] - \sqrt{b_k^2-1}E_3\Big[\bar{\tau}(\sqrt{\bar{n}_d^2-1} + \sqrt{b_k^2-1})\Big]}{\bar{\tau}\bar{n}_d^2/\sqrt{\bar{n}_d^2-1}} \\
& + \frac{\sqrt{a_k^2-1}E_4\Big[\bar{\tau}(\sqrt{\bar{n}_d^2-1} + \sqrt{a_k^2-1})\Big] - \sqrt{b_k^2-1}E_4\Big[\bar{\tau}(\sqrt{\bar{n}_d^2-1} + \sqrt{b_k^2-1})\Big]}{\bar{\tau}\bar{n}_d^2}\Bigg\},
\end{aligned}
\tag{30}
$$

where $\bar{n}_k$ is the refractive index value at the center of mesh k, and $a_k = \frac{1}{2}(\bar{n}_k + \bar{n}_{k+1})$, $b_k = \frac{1}{2}(\bar{n}_k + \bar{n}_{k-1})$.

Similarly, I_{0p2} can be expressed as

$$
I_{0p2} = \frac{n_2^2\sigma}{\pi}\sum_{k=1}^{N} C_k T_k^4, \tag{31}
$$

where $T_1 = T_{t2}$, $T_N = T_{t1}$, $C_1 = \varepsilon_2$, $C_N = 0$. And for $2 \leqslant k \leqslant N-1$, C_k is

$$
\begin{aligned}
C_k = 2(1-\varepsilon_2)\Bigg\{ & \frac{(a_k-1)E_4\Big[\bar{\tau}(a_k-1)\Big] - (b_k-1)E_4\Big[\bar{\tau}(b_k-1)\Big]}{\bar{\tau}} - a_kE_3\Big[\bar{\tau}(a_k-1)\Big] + b_kE_3\Big[\bar{\tau}(b_k-1)\Big] \\
& + \frac{E_5\Big[\bar{\tau}(a_k-1)\Big] - E_5\Big[\bar{\tau}(b_k-1)\Big]}{\bar{\tau}^2} - \frac{\sqrt{a_k^2-1}E_4\Big(\bar{\tau}\sqrt{a_k^2-1}\Big) - \sqrt{b_k^2-1}E_4\Big(\bar{\tau}\sqrt{b_k^2-1}\Big)}{\bar{\tau}} \\
& - \frac{E_5\Big(\bar{\tau}\sqrt{a_k^2-1}\Big) - E_5\Big(\bar{\tau}\sqrt{b_k^2-1}\Big)}{\bar{\tau}^2}\Bigg\}.
\end{aligned}
\tag{32}
$$

The solutions could be obtained from Eqs. (29) and (31) as

$$T_{\mathrm{p1}}^4 = \sum_{k=1}^{N} \frac{A_k + C_k(1-\varepsilon_1)k_2/\bar{n}^2(d)}{1-K_1(1-\varepsilon_1)} T_k^4, \tag{33}$$

$$T_{\mathrm{p2}}^4 = \sum_{k=1}^{N} \frac{C_k + A_k(1-\varepsilon_2)k_1\bar{n}^2(d)}{1-K_2(1-\varepsilon_2)} T_k^4. \tag{34}$$

For a constant refractive index, the following expressions can be derived:

$$A_k = 2(1-\varepsilon_1)\left\{E_3\left[\kappa d - \kappa\left(k+\frac{1}{2}\right)\Delta z\right] - E_3\left[\kappa d - \kappa\left(k-\frac{1}{2}\right)\Delta z\right]\right\}, \tag{35}$$

$$C_k = 2(1-\varepsilon_2)\left\{E_3\left[\kappa\left(k-\frac{1}{2}\right)\Delta z\right] - E_3\left[\kappa\left(k+\frac{1}{2}\right)\Delta z\right]\right\}, \tag{36}$$

$$k_1 = k_2 = 2E_3(\kappa d), \tag{37}$$

$$K_1 = 4(1-\varepsilon_2)E_3^2(\kappa d), \tag{38}$$

$$K_2 = 4(1-\varepsilon_1)E_3^2(\kappa d). \tag{39}$$

In the medium with a linear refractive index, the radiative flux at point z_j would be given as

$$q_j = 2\sigma n_j^2 \sum_{k=1}^{N} B'_{kj} T_k^4, \tag{40}$$

where $T_1 = T_{\mathrm{p2}}$, $T_N = T_{\mathrm{p1}}$. And it can also be written as

$$q_j = \sum_{k=2}^{N-1} \left(B'_{kj} + B'_{1j}C'_k + B'_{Nj}A'_k\right) T_k^4 + (B'_{1j}C'_1 + B'_{Nj}A'_1)T_{\mathrm{b2}}^4 + (B'_{1j}C'_N + B'_{Nj}A'_N)T_{\mathrm{b1}}^4. \tag{41}$$

For the case of a linear refractive index, B'_{kj} has been deduced in [6].

3.4. Results and discussion on radiative flux at radiative equilibrium

The results of radiative flux at radiative equilibrium are presented in a reduced form as $q_{\mathrm{r}} = 4q_j/(n_1+n_2)^2$ for a linear refractive index distribution or $q_{\mathrm{r}} = q_j/n^2$ for constant refractive index [6]. The results of reduced radiative flux in medium with a constant optical thickness and black boundaries are shown in Fig. 3, wherein eight linear refractive index distributions and a constant one are considered. It should be pointed out that the results for the linear refractive index distribution of $n_1 = 1.8$, $n_2 = 1.2$ and for a constant refractive index have also been presented in [6]. The corresponding results in this paper and that reported in [6] exactly agree with each other. It is easy to see, in Fig. 3, that the radiative flux inside a one-dimensional semitransparent slab is significantly influenced by the refractive index distribution, but with a linear refractive index, it keeps constant for the fixed values of n_1 and n_2, and does not change when the values of n_1 and n_2 are interchanged.

The influences of optical thickness κd and the boundary emissivities on the radiative flux at radiative equilibrium are shown in Fig. 4. The results for both of the linear refractive indexes and the corresponding constant refractive index are shown in Fig. 4. Comparisons with the results in [6] are presented in Fig. 4(a) for black boundaries considered, and exact agreements are shown for the cases of $\kappa d = 0.01,\ 0.1,\ 1$ and 10. The radiative flux monotonously decreases with increasing optical thickness, the refractive index being constant or linearly distributed, and it is independent of boundary emissivities. For any optical thickness, however, the radiative flux can be greatly influenced by the refractive index, and the effect of refractive index closely relates to the two boundary emissivities. When the two boundary emissivities are same, see Figs. 4(b) and (c), the radiative flux keeps constant as the values of n_1 and n_2 of a linear refractive index distribution are interchanged, though the temperature distribution in medium changes greatly [11]. For two different but respectively constant boundary emissivities, comparing curve 2 with curve 3 in Fig. 4(d) or (e), the radiative flux changes greatly as the values of n_1 and n_2 changed. When the values of n_1 and n_2 are interchanged along with the interchanging of the two boundary emissivities, however, the radiative flux keeps constant, as compared curve 2 in Fig. 4(d) with curve 3 in Fig. 4(e) or curve 3 in Fig. 4(d) with curve 2 in Fig. 4(e).

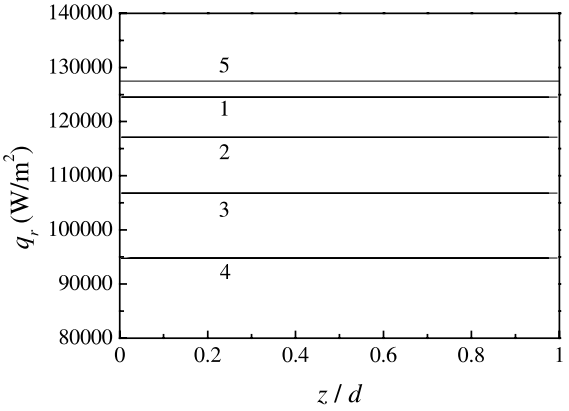

Fig. 3. Reduced radiative flux at radiative equilibrium inside a slab with a constant optical thickness ($T_{b1} = 1500$ K and $T_{b2} = 1000$ K; $\kappa d = 1$; $\varepsilon_1 = \varepsilon_2 = 1.0$; curves: 1. $n_1 = 1.6$, $n_2 = 1.4$ or $n_1 = 1.4$, $n_2 = 1.6$; 2. $n_1 = 1.7$, $n_2 = 1.3$ or $n_1 = 1.3$, $n_2 = 1.7$; 3. $n_1 = 1.8$, $n_2 = 1.2$ or $n_1 = 1.2$, $n_2 = 1.8$; 4. $n_1 = 1.9$, $n_2 = 1.1$ or $n_1 = 1.1$, $n_2 = 1.9$; $n_1 = n_2 = 1.5$).

4. Simultaneous radiative and conductive heat transfer in medium

4.1. Governing equation and discretized solution

At steady-state, the divergence of the heat flux in medium equals zero. For the simultaneous radiation and conduction heat transfer, it can be written as

$$\operatorname{div}(q_r + q_c) = 0, \tag{42}$$

where q_r and q_c are the heat fluxes transferred by radiation and conduction, respectively. For an one-dimensional problem, the divergences of them will be

$$\operatorname{div} q_r = \kappa\left[4n^2(z)\sigma T^4(z) - 2\pi\int_{\mu=0}^{1}[I_m(z,\mu) + I_m(z,-\mu)]\,d\mu\right], \tag{43}$$

$$\operatorname{div} q_c = -\lambda\frac{d^2T}{dz^2}. \tag{44}$$

The discrete form of Eq. (43) could be

$$\begin{aligned}\operatorname{div} q_r = 4\kappa\sigma n_j^2\Bigg[&\left(1 - \frac{B_{1j}C'_j}{2} - \frac{B_{Nj}A'_j}{2} - \frac{B_{jj}}{2}\right)T_j^4 - \frac{B_{1j}C'_1 + B_{Nj}A'_1}{2}T_{b2}^4 - \frac{B_{1j}C'_N + B_{Nj}A'_N}{2}T_{b1}^4 \\ &- \sum_{k=2}^{j-1}\frac{B_{1j}C'_k + B_{Nj}A'_k + B_{kj}}{2}T_k^4 - \sum_{k=j+1}^{N-1}\frac{B_{1j}C'_k + B_{Nj}A'_k + B_{kj}}{2}T_k^4\Bigg],\end{aligned} \tag{45}$$

where the coefficients B_{kj} have been presented in [7]. By the finite difference method, Eq. (44) can be discretized as

$$\begin{aligned}&\operatorname{div} q_c = \lambda\frac{12T_2 - 8T_{b2} - 4T_3}{3\Delta z^2} \quad \text{for } j = 2,\\ &\operatorname{div} q_c = \lambda\frac{2T_j - T_{j-1} - T_{j+1}}{\Delta z^2} \quad \text{for } 3 \leqslant j \leqslant N-2,\\ &\operatorname{div} q_c = \lambda\frac{12T_{N-1} - 4T_{N-2} - 8T_{b1}}{3\Delta z^2} \quad \text{for } j = N-1.\end{aligned} \tag{46}$$

Substituting Eqs. (45) and (46) into Eq. (42), we get the discrete energy equation of the simultaneous radiation and conduction in medium. By linearizing T_j^4 in Eq. (45), and solving the algebraic equation set by an iterative solution, the temperature T_j induced by the simultaneous radiation and conduction in medium can be finally obtained, and then, the radiative flux of the simultaneous radiation and conduction heat transfer can be determined from Eq. (41).

4.2. Temperature and radiative flux of simultaneous radiation and conduction

Based on the deduction above, the steady-state simultaneous radiation and conduction heat transfer in a slab of semitransparent medium is solved as follows. The thickness of the slab keeps a constant value of 1 cm, and the two boundary temperatures are $T_{b1} = 1500$ K and $T_{b2} = 1000$ K, respectively. Four couples of medium thermal conductivity and absorptive coefficient combinations are considered. For each combination, a constant and two linear refractive index distributions are discussed. The values of n_1 and n_2 of a linear refractive index distribution are interchanged to obtain the other linear refractive index distribution, and the constant refractive index is the mean value

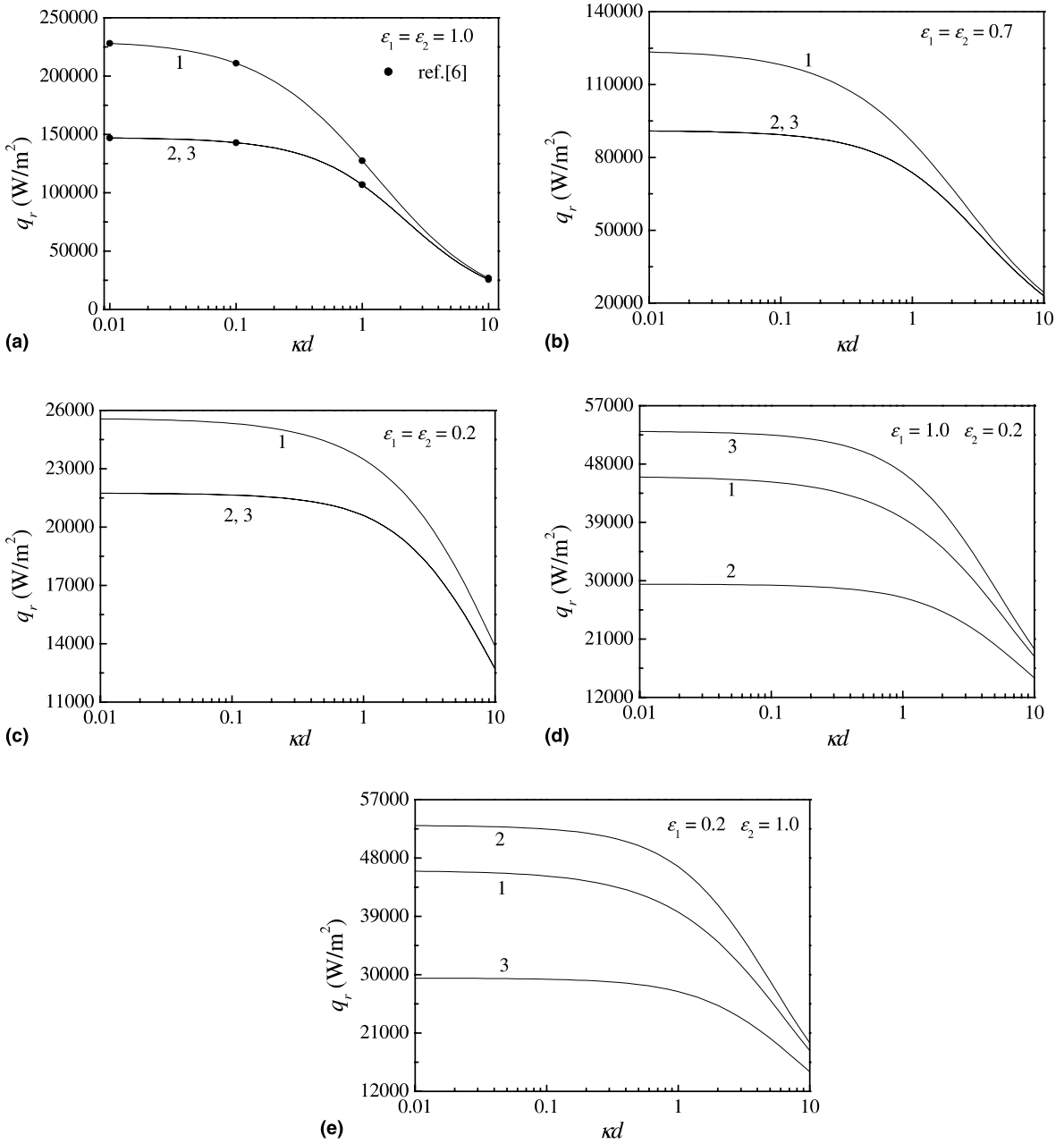

Fig. 4. Effects of optical thickness and refractive index distribution on the reduced radiative flux at radiative equilibrium ($T_{b1} = 1500$, $T_{b2} = 1000$; curves: 1. $n = 1.5$; 2. $n_1 = 1.8$, $n_2 = 1.2$; 3. $n_1 = 1.2$, $n_2 = 1.8$).

of n_1 and n_2. Both black and gray boundary walls are considered for each case above. The temperature and radiative flux results are shown in Figs. 5 and 6, respectively. It is necessary to point out that, the results for the medium with two black boundaries and a linear refractive index distribution of $n_1 > n_2$ or a constant one have been presented also in [6], and the results agree well each other, see Fig. 4(1) for example.

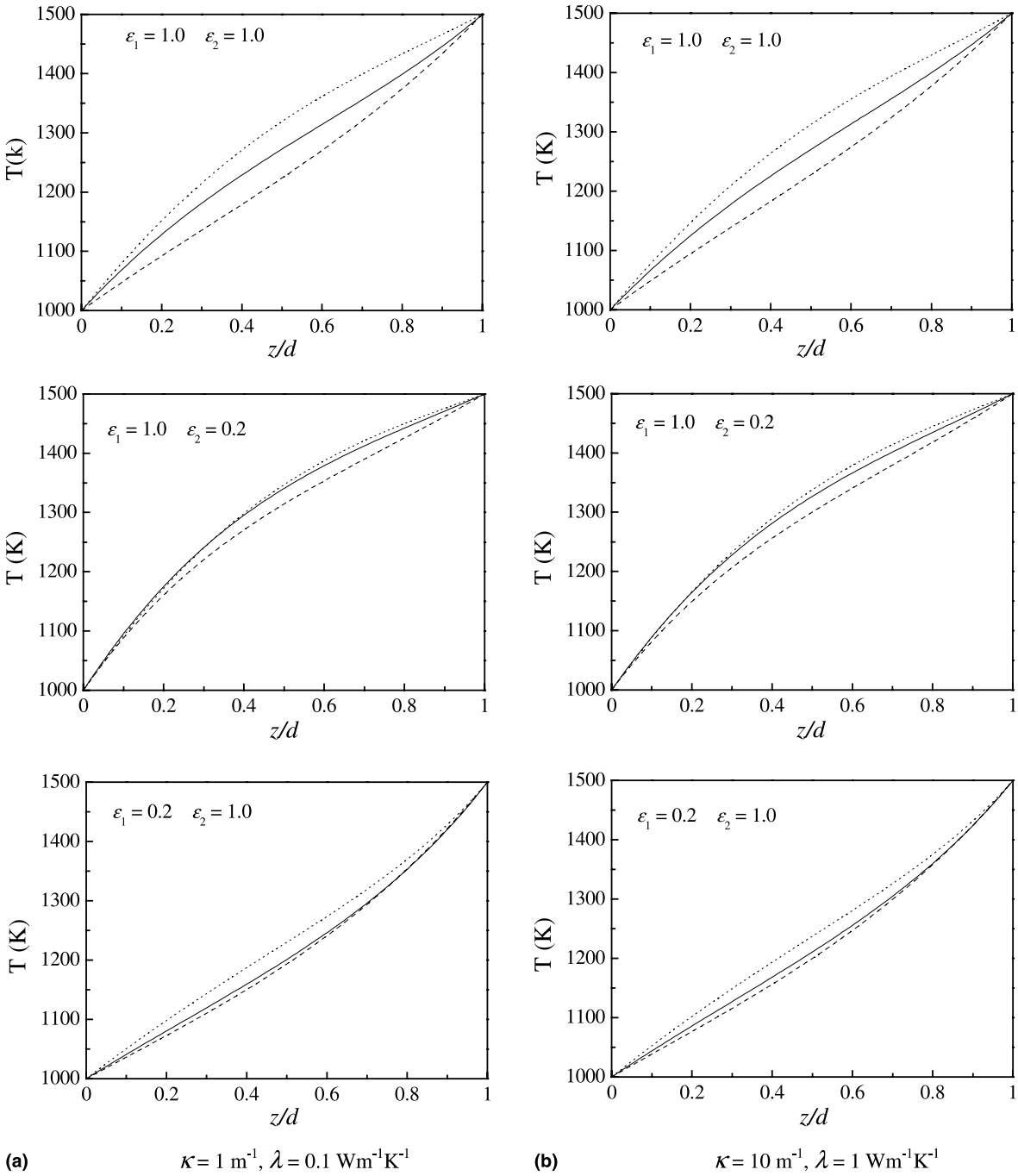

Fig. 5. Temperature distribution of the simultaneous radiation and conduction heat transfer in a slab ($T_{b1} = 1500$ and $T_{b2} = 1000$; solid lines: $n = 1.5$; dotted lines: $n_1 = 1.8$, $n_2 = 1.2$; dashed lines: $n_1 = 1.2$, $n_2 = 1.8$).

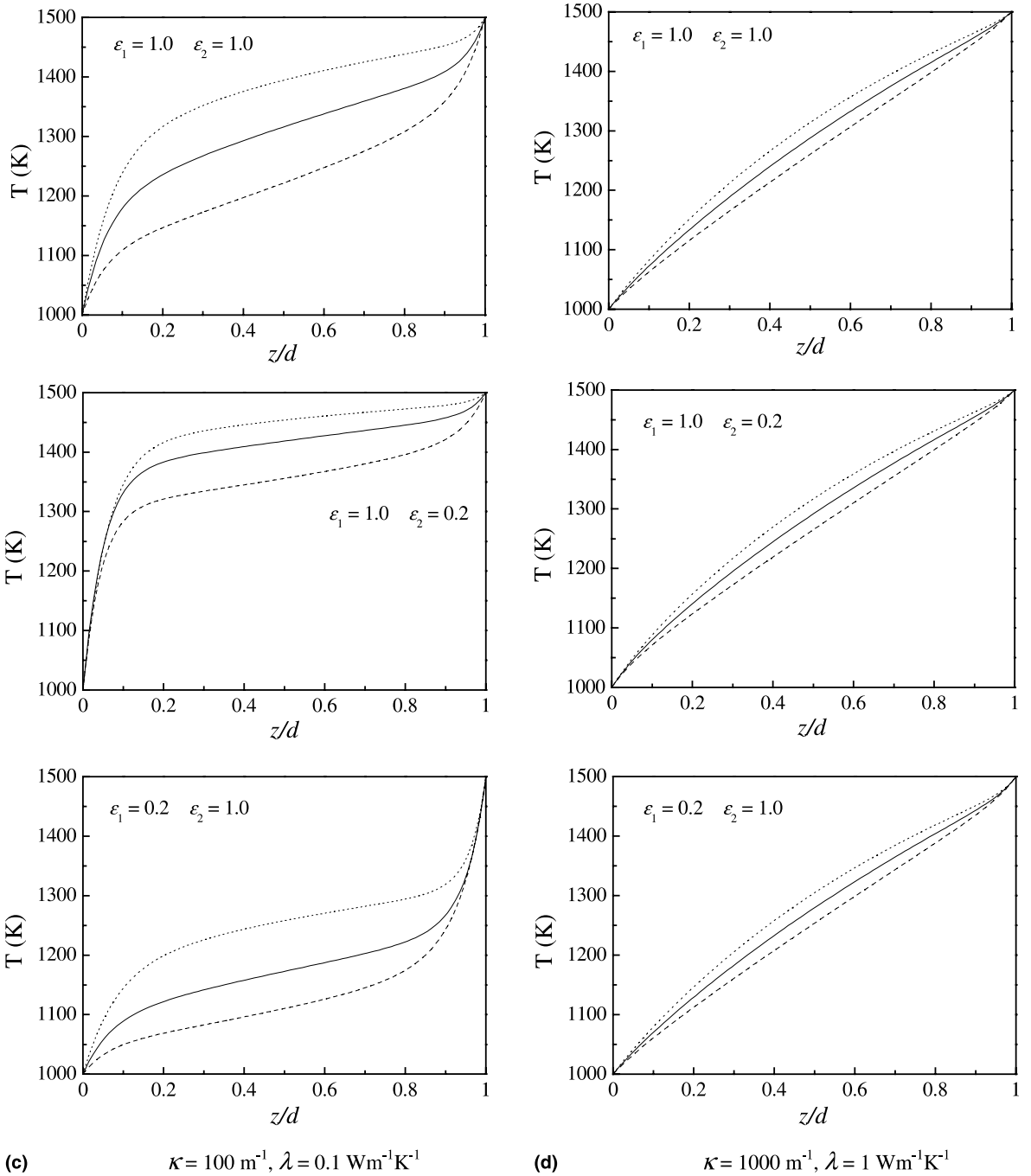

Fig. 5 (*continued*)

Fig. 5 shows that, the combination of thermal conductivity and absorptive coefficient, the refractive index distribution and the wall emissivities have significant influences on the temperature distribution in medium. Increasing the wall emissivity of the high temperature boundary and/or decreasing that of the low temperature boundary can increase the temperature level in medium. The influence of boundary wall emissivities on temperature distribution is very obvious for a moderate absorptive coefficient and a small thermal conductivity combination (Fig. 5(c)), and becomes almost neglectable for high absorptive coefficient coupled with not very small thermal conductivity (Fig. 5(d)).

The temperature in the medium with $n_1 > n_2$ is higher than that with $n_1 < n_2$, and the temperature curve in the medium with a constant refractive index of the mean value of n_1 and n_2 locates between the two temperature curves (Figs. 5(a)–(d)). It may be explained as the total reflection inside the medium differing under different linear refractive index. Because of the total reflection inside medium, for the case $n_1 > n_2$, the higher temperature boundary (boundary 1) has greater influences not only on the downward radiation transfer from boundary 1 toward boundary 2, but also on the upward radiation transfer from boundary 2 toward boundary 1, and thus, the temperature level heightens. Similarly, the linear refractive index with $n_1 < n_2$ will enhance the influence of low temperature boundary (boundary 2) on radiation transfer and results in the drop of temperature level.

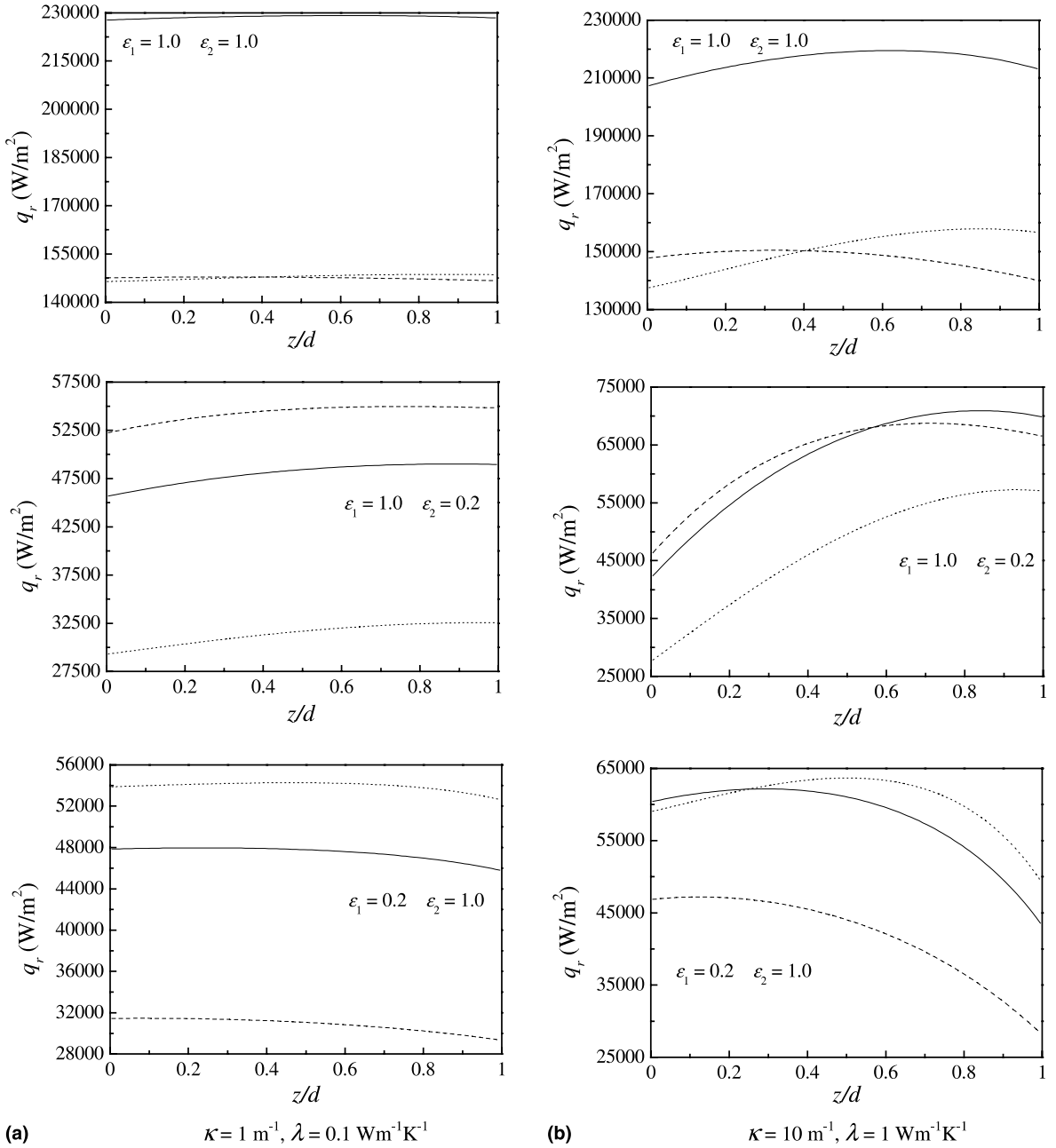

Fig. 6. Reduced radiative flux distribution of simultaneous radiation and conduction heat transfer in a slab ($T_{b1} = 1500$ and $T_{b2} = 1000$; solid lines: $n = 1.5$; dotted lines: $n_1 = 1.8$, $n_2 = 1.2$; dashed lines: $n_1 = 1.2$, $n_2 = 1.8$).

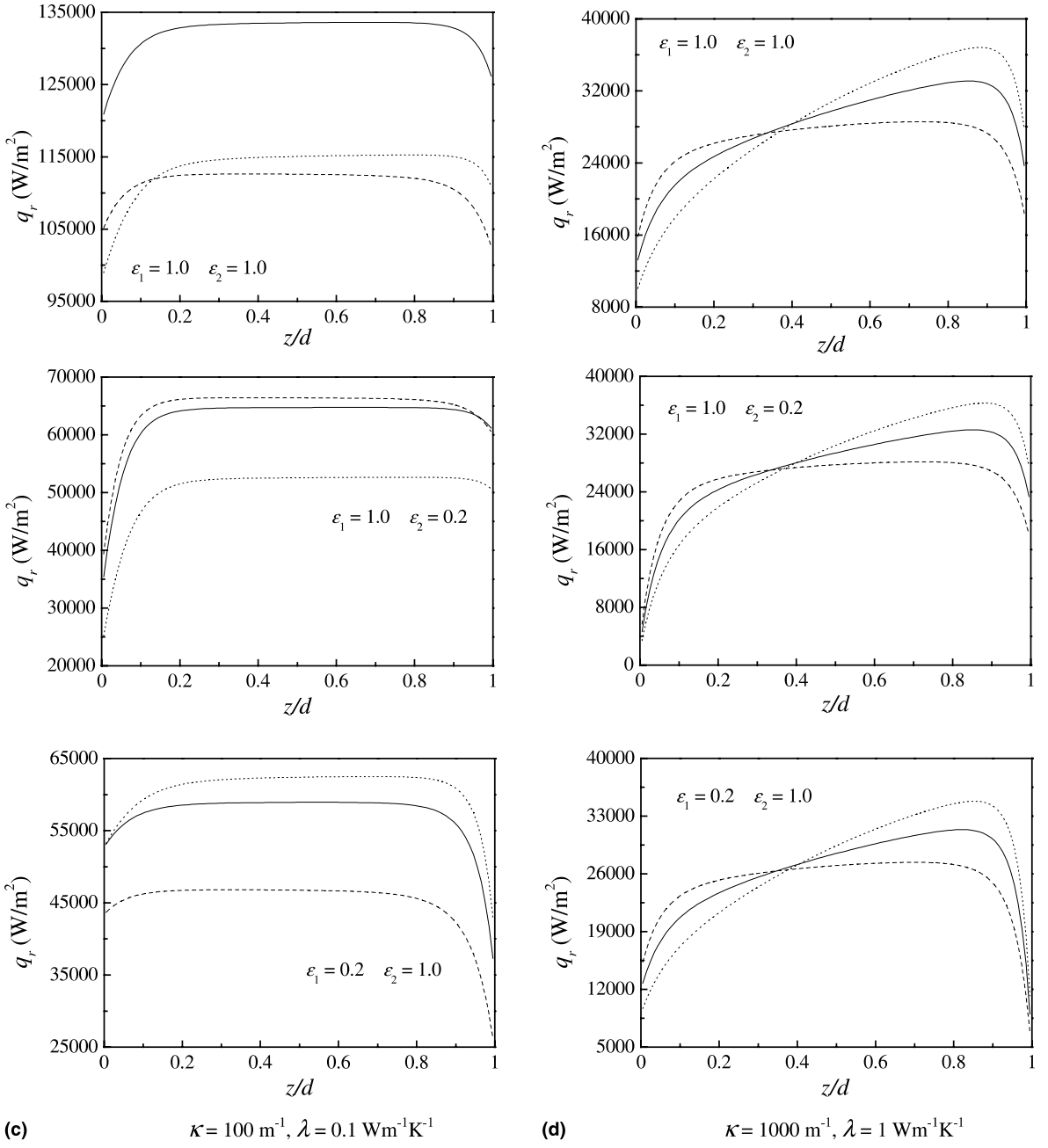

Fig. 6 (*continued*)

As shown in Fig. 6, the radiative flux distribution in medium shows complicated dependency on the combination of thermal conductivity and absorptive coefficient, the refractive index distribution and the wall emissivities. When the thermal conductivity and absorptive coefficient are both small, the radiative flux varies slightly and is somewhat like the distribution at radiative equilibrium (Fig. 6(a)). For the combination of a small thermal conductivity and a moderate absorptive coefficient, the radiative flux distribution is almost flat in the central region of the medium (see Fig. 6(c)). As the thermal conductivity increases, the coupling effect of radiation and conduction becomes obvious, and the radiative flux distribution changes greatly in the whole region of the medium.

5. Conclusions

By using the curved ray tracing technique in combination with the pseudo-source adding method, an exact expression of the radiative flux in semitransparent medium is deduced. The simultaneous radiation and conduction heat transfer in a linear refractive index medium with diffuse and gray boundary walls is solved. The conclusions can be drawn as following:

(i) The refractive index distribution, absorbing coefficient, thermal conductivity and the boundary wall emissivities are combined to significantly influence the radiative flux and temperature distributions in the medium.
(ii) The radiative flux distribution of a simultaneous radiation and conduction in the medium differs greatly from that at equilibrium. The latter is constant in medium for a given case, while the former usually varies nonlinearly.
(iii) Compared with the effect of a constant refractive index, a linear refractive index can either heighten or lower the temperature in medium.
(iv) The influence of boundary wall emissivities on temperature distribution is very significant under a moderate absorptive coefficient and a small thermal conductivity combination, and becomes almost neglectable under a great absorptive coefficient and a not very small thermal conductivity.

Acknowledgements

The project is financially supported by the National Natural Science Foundation of China (Grant No. 50076010), and the Multidiscipline Scientific Research Foundation of Harbin Institute of Technology (Grant No. HIT.MD2000.16).

References

[1] C.M. Spuckler, R. Siegel, Refractive index and scattering effects on radiative behavior of a semitransparent layer, J. Thermophys. Heat Transfer 7 (2) (1993) 302–310.
[2] R. Siegel, Refractive index effects on local radiative emission from a rectangular semitransparent solid, J. Thermophys. Heat Transfer 8 (3) (1994) 625–628.
[3] R. Siegel, C.M. Spuckler, Variable refractive index effects on radiation in semitransparent scattering multilayered regions, J. Thermophys. Heat Transfer 7 (4) (1993) 624–630.
[4] H.P. Tan, P.Y. Wang, X.L. Xia, Transient coupled radiation and conduction in an absorbing and scattering composite layer, AIAA J. Thermophys. Heat Transfer 14 (1) (2000) 77–87.
[5] Y.T. Qiao, in: Graded Index Optics, Science Press, Beijing, 1991, pp. 1–8 (in Chinese).
[6] P. Ben Abdallah, V. Le Dez, Radiative flux field inside an absorbing–emitting semitransparent slab with variable spatial refractive index at radiative conductive coupling, J. Quant. Spectrosc. Radiat. Transfer 67 (2) (2000) 125–137.
[7] P. Ben Abdallah, V. Le Dez, Temperature field inside an absorbing–emitting semitransparent slab at radiative equilibrium with variable spatial refractive index, J. Quant. Spectrosc. Radiat. Transfer 65 (4) (2000) 595–608.
[8] P. Ben Abdallah, V. Le Dez, Thermal emission of a semitransparent slab with variable spatial refractive index, J. Quant. Spectrosc. Radiat. Transfer 67 (3) (2000) 185–198.
[9] P. Ben Abdallah, V. Le Dez, Thermal emission of a two-dimensional rectangular cavity with spatial affine refractive index, J. Quant. Spectrosc. Radiat. Transfer 66 (6) (2000) 555–569.
[10] Y. Huang, X.L. Xia, H.P. Tan, et al., Apparent emitting properties of a semi-transparent medium layer with specular semi-transparent surface and diffuse substrate, Acta Energiae Solaris Sinica 20 (2) (1999) 116–121 (in Chinese).
[11] Y. Huang, X.L. Xia, H.P. Tan, Temperature fields inside an absorbing–emitting semi-transparent slab at radiative equilibrium with linear graded index and gray walls, J. Quant. Spectrosc. Radiat. Transfer (in press).